International Telecommunication Union

ITU-R

Radiocommunication Sector of ITU

Recommendation ITU-R P.833-8

(09/2013)

Attenuation in vegetation

P Series

Radiowave propagation

International Telecommunication Union

Foreword

The role of the Radiocommunication Sector is to ensure the rational, equitable, efficient and economical use of the radio-frequency spectrum by all radiocommunication services, including satellite services, and carry out studies without limit of frequency range on the basis of which Recommendations are adopted.

The regulatory and policy functions of the Radiocommunication Sector are performed by World and Regional Radiocommunication Conferences and Radiocommunication Assemblies supported by Study Groups.

Policy on Intellectual Property Right (IPR)

ITU-R policy on IPR is described in the Common Patent Policy for ITU-T/ITU-R/ISO/IEC referenced in Annex 1 of Resolution ITU-R 1. Forms to be used for the submission of patent statements and licensing declarations by patent holders are available from http://www.itu.int/ITU-R/go/patents/en where the Guidelines for Implementation of the Common Patent Policy for ITU-T/ITU-R/ISO/IEC and the ITU-R patent information database can also be found.

Series of ITU-R Recommendations

(Also available online at http://www.itu.int/publ/R-REC/en)

Series	Title
BO	Satellite delivery
BR	Recording for production, archival and play-out; film for television
BS	Broadcasting service (sound)
BT	Broadcasting service (television)
F	Fixed service
M	Mobile, radiodetermination, amateur and related satellite services
P	**Radiowave propagation**
RA	Radio astronomy
RS	Remote sensing systems
S	Fixed-satellite service
SA	Space applications and meteorology
SF	Frequency sharing and coordination between fixed-satellite and fixed service systems
SM	Spectrum management
SNG	Satellite news gathering
TF	Time signals and frequency standards emissions
V	Vocabulary and related subjects

Note: *This ITU-R Recommendation was approved in English under the procedure detailed in Resolution ITU-R 1.*

Electronic Publication
Geneva, 2013

RECOMMENDATION ITU-R P.833-8

Attenuation in vegetation

(Question ITU-R 202/3)

(1992-1994-1999-2001-2003-2005-2007-2012-2013)

Scope

This Recommendation presents several models to enable the reader to evaluate the effect of vegetation on radiowave signals. Models are presented that are applicable to a variety of vegetation types for various path geometries suitable for calculating the attenuation of signals passing through vegetation. The Recommendation also contains measured data of vegetation fade dynamics and delay spread characteristics.

The ITU Radiocommunication Assembly,

considering

that attenuation in vegetation can be important in several practical applications,

recommends

that the content of Annex 1 be used for evaluating attenuation through vegetation between 30 MHz and 60 GHz.

Annex 1

1 Introduction

Attenuation in vegetation can be important in some circumstances, for both terrestrial and Earth-space systems. However, the wide range of conditions and types of foliage makes it difficult to develop a generalized prediction procedure. There is also a lack of suitably collated experimental data.

The models described in the following sections apply to particular frequency ranges and for different types of path geometry.

2 Obstruction by woodland

2.1 Terrestrial path with one terminal in woodland

For a terrestrial radio path where one terminal is located within woodland or similar extensive vegetation, the additional loss due to vegetation can be characterized on the basis of two parameters:

– the specific attenuation rate (dB/m) due primarily to scattering of energy out of the radio path, as would be measured over a very short path;

– the maximum total additional attenuation due to vegetation in a radio path (dB) as limited by the effect of other mechanisms including surface-wave propagation over the top of the vegetation medium and forward scatter within it.

In Fig. 1, the transmitter is outside the woodland and the receiver is a certain distance, d, within it. The excess attenuation, A_{ev}, due to the presence of the vegetation is given by:

$$A_{ev} = A_m [1 - \exp (- d \gamma / A_m)] \quad (1)$$

where:

d: length of path within woodland (m)

γ: specific attenuation for very short vegetative paths (dB/m)

A_m: maximum attenuation for one terminal within a specific type and depth of vegetation (dB).

FIGURE 1

Representative radio path in woodland

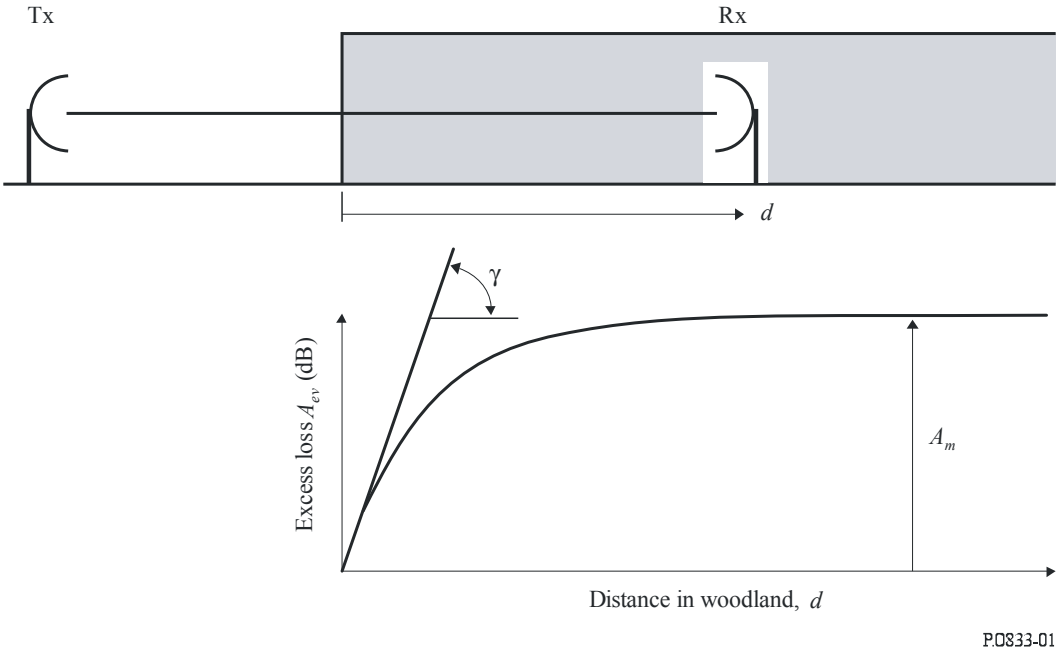

It is important to note that excess attenuation, A_{ev}, is defined as excess to all other mechanisms, not just free space loss. Thus if the radio path geometry in Fig. 1 were such that full Fresnel clearance from the terrain did not exist, then A_{ev} would be the attenuation in excess of both free-space and diffraction loss. Similarly, if the frequency were high enough to make gaseous absorption significant, A_{ev} would be in excess of gaseous absorption.

It may also be noted that A_m is equivalent to the clutter loss often quoted for a terminal obstructed by some form of ground cover or clutter.

The value of specific attenuation due to vegetation, γ dB/m, depends on the species and density of the vegetation. Approximate values are given in Fig. 2 as a function of frequency.

Figure 2 shows typical values for specific attenuation derived from various measurements over the frequency range 30 MHz to about 30 GHz in woodland. Below about 1 GHz there is a tendency for vertically polarized signals to experience higher attenuation than horizontally, this being thought due to scattering from tree-trunks.

FIGURE 2

Specific attenuation due to woodland

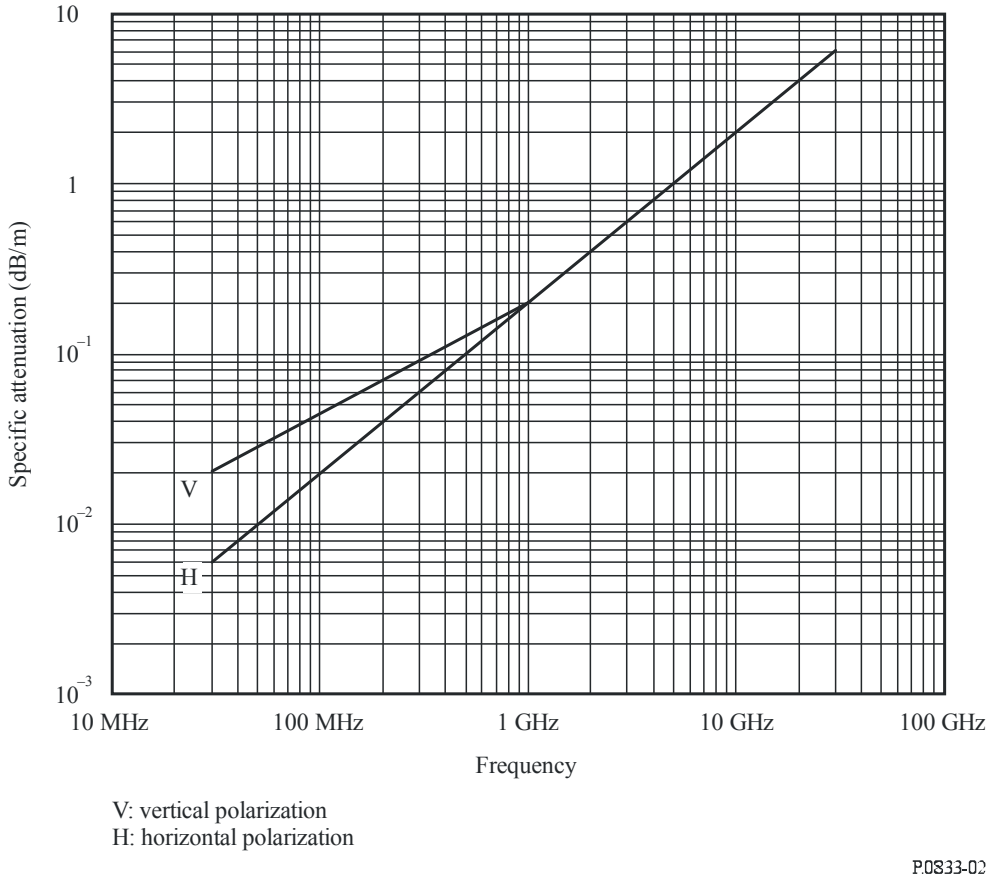

V: vertical polarization
H: horizontal polarization

P.0833-02

It is stressed that attenuation due to vegetation varies widely due to the irregular nature of the medium and the wide range of species, densities, and water content obtained in practice. The values shown in Fig. 2 should be viewed as only typical.

At frequencies of the order of 1 GHz the specific attenuation through trees in leaf appears to be about 20% greater (dB/m) than for leafless trees. There can also be variations of attenuation due to the movement of foliage, such as due to wind.

The maximum attenuation, A_m, as limited by scattering from the surface wave, depends on the species and density of the vegetation, plus the antenna pattern of the terminal within the vegetation and the vertical distance between the antenna and the top of the vegetation.

Measurements in the frequency range 105-2 200 MHz carried out in mixed coniferous-deciduous vegetation (mixed forest) near St. Petersburg (Russia) on paths varying in length from a few hundred meters to 7 km with various species of trees of mean height 16 m. These were found to agree on average with equation (1) with constants for specific and maximum attenuation as given in Table 1.

TABLE 1

Parameter	**Frequency (MHz) and polarization**				
Frequency, MHz	105.9 Horizontal	466.475 Slant	949.0 Slant	1852.2 Slant	2117.5 Slant
γ (dB/m)	0.04	0.12	0.17	0.30	0.34
A_m (dB)	9.4	18.0	26.5	29.0	34.1

A frequency dependence of A_m (dB) of the form:

$$A_m = A_1 f^{\alpha} \tag{2}$$

where f is the frequency (MHz) has been derived from various experiments:

- Measurements in the frequency range 900-1 800 MHz carried out in a park with tropical trees in Rio de Janeiro (Brazil) with a mean tree height of 15 m have yielded $A_1 = 0.18$ dB and $\alpha = 0.752$. The receiving antenna height was 2.4 m.
- Measurements in the frequency range 900-2 200 MHz carried out in a forest near Mulhouse (France) on paths varying in length from a few hundred metres to 6 km with various species of trees of mean height 15 m have yielded $A_1 = 1.15$ dB and $\alpha = 0.43$. The receiving antenna in woodland was a $\lambda/4$ monopole mounted on a vehicle at a height of 1.6 m and the transmitting antenna was a $\lambda/2$ dipole at a height of 25 m. The standard deviation of the measurements was 8.7 dB. Seasonal variations of 2 dB at 900 MHz and 8.5 dB at 2 200 MHz were observed.
- Measurements in the frequency range 105.9-2 117.5 MHz carried out in two forest-park areas with coniferous-deciduous vegetation (mixed forest) in St. Petersburg (Russia) with a tree height of 12 to 16 m and average distance between them was approximately 2 to 3 m, that corresponds to the density of 20-10 tree/100 m^2 have yielded $A_1 = 1.37$ dB and $\alpha = 0.42$. To receive the signal, a quarter-wave length dipole antenna at 1.5 m above the ground level was used. The distance between the receiver and the transmitter antenna was 0.4 to 7 km, and paths for measurement were chosen so as to have line-of-sight between these antennas without any obstacles but only the woodland to be measured. Different phases of the experiment were performed in similar weather conditions: dry weather, wind speed 0 to 7 m/s.

2.2 Satellite slant paths

Representative radio path in woodland:

In Fig. 3, Transmitter (TX) and Receiver (RX) are outside the woodland. The relevant parameters are:

- vegetation path length, d;
- average tree height, h_v;
- height of the Rx antenna over ground, h_a;
- radio path elevation, θ;
- distance of the antenna to the roadside woodland, d_w.

FIGURE 3

Representative radio path in woodland with vegetation path length, *d*, average tree height, h_v, height of the Rx antenna over ground, h_a, radio path elevation, θ, and distance of the antenna to the roadside woodland, d_w

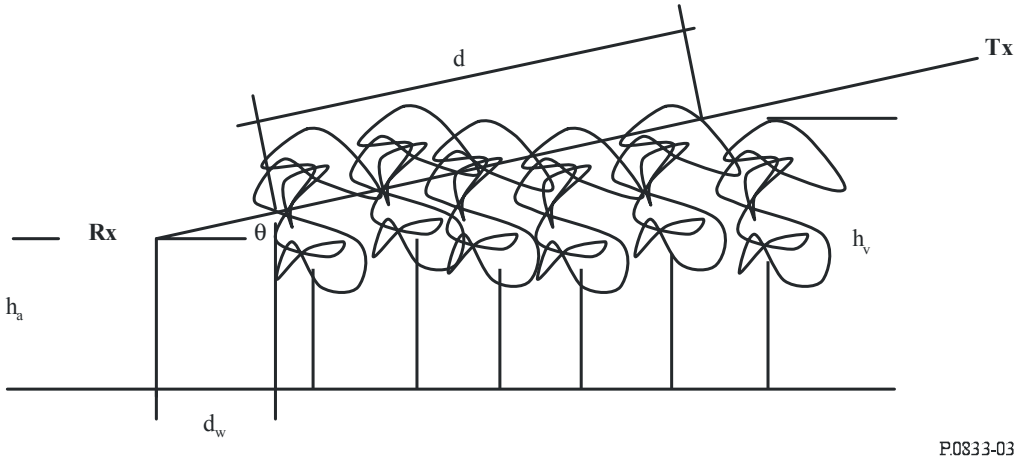

To describe the attenuation loss, L along both, horizontal and slant foliage path propagation, the following model is proposed:

$$L(\text{dB}) = A f^B d^C (\theta + E)^G \quad (3)$$

where:

f: frequency (MHz)

d: vegetation depth (m)

θ: elevation (degrees)

A, B, C, E, and G: empirical found parameters.

A fit to measurements made in pine woodland in Austria gave:

$$L(\text{dB}) = 0.25 f^{0.39} d^{0.25} \theta^{0.05} \quad (4)$$

3 Single vegetative obstruction

3.1 At or below 1 GHz

Equation (1) does not apply for a radio path obstructed by a single vegetative obstruction where both terminals are outside the vegetative medium, such as a path passing through the canopy of a single tree. At VHF and UHF, where the specific attenuation has relatively low values, and particularly where the vegetative part of the radio path is relatively short, this situation can be modelled on an approximate basis in terms of the specific attenuation and a maximum limit to the total excess loss:

$$A_{et} = d \gamma \quad (5)$$

where:

d: length of path within the tree canopy (m)

γ: specific attenuation for very short vegetative paths (dB/m)

and $A_{et} \leq$: lowest excess attenuation for other paths (dB).

The restriction of a maximum value for A_{et} is necessary since, if the specific attenuation is sufficiently high, a lower-loss path will exist around the vegetation. An approximate value for the minimum attenuation for other paths can be calculated as though the tree canopy were a thin finite-width diffraction screen using the method of Recommendation ITU-R P.526.

It is stressed that equation (5), with the accompanying maximum limit on A_{et}, is only an approximation. In general it will tend to overestimate the excess loss due to the vegetation. It is thus most useful for an approximate evaluation of additional loss when planning a wanted service. If used for an unwanted signal it may significantly underestimate the resulting interference.

3.2 Above 1 GHz

For terrestrial paths, the method based on RET described in § 3.2.1 should be applied to compute the effect of a single tree.

For slant paths, the method based on multiple scattering theory described in § 3.2.2 should be applied to compute the effect of a single tree.

3.2.1 Terrestrial path

In order to estimate the total field, the diffracted, ground reflected and through-vegetation scattering components are first calculated and then combined.

The diffracted components consist of those over the top of the vegetation and those around the sides of the vegetation. These components and the ground reflected component are calculated using ITU-R Recommendations. The through or scattered component is calculated using a model based upon the theory of radiative energy transfer (RET).

3.2.1.1 Calculation of the top diffracted component

The diffraction loss, L_{top}, experienced by the signal path diffracted over the vegetation, may be treated as double isolated knife-edge diffraction for the geometry defined in Fig. 4.

FIGURE 4

Component diffracted over top of vegetation

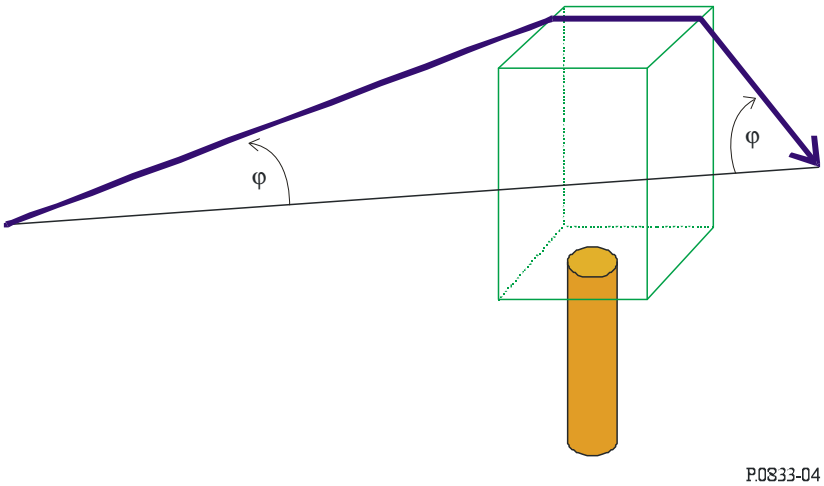

This is calculated as follows:

$$L_{top} = L_{top\_diff} + G_{Tx}(\varphi) + G_{Rx}(\varphi) \quad (6)$$

where $G_{Tx}(\varphi)$ and $G_{Rx}(\varphi)$ are the losses due to angles of the diffracted wave leaving the transmit antenna and coming into the receive antenna, respectively. L_{top_diff} is the total diffraction loss as calculated using the method of Recommendation ITU-R P.526 for double isolated edges.

3.2.1.2 Calculation of the side diffracted component

The diffraction loss, L_{sidea} and L_{sideb}, experienced by the signal diffracted around the vegetation, may again be treated as double isolated knife-edge diffraction, for the geometry defined in Fig. 5.

FIGURE 5

Components diffracted around the vegetation

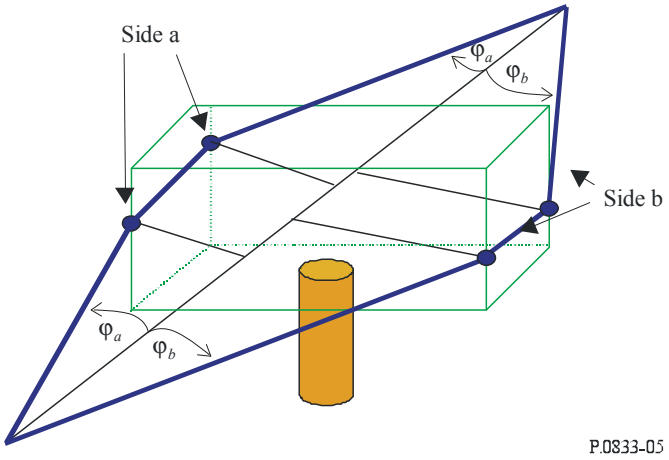

The losses are calculated using equations (7) and (8).

$$L_{sidea} = L_{diff\_sidea} + G_{Tx}(\varphi_a) + G_{Rx}(\varphi_a) \quad (7)$$

and

$$L_{sideb} = L_{diff\_sideb} + G_{Tx}(\varphi_b) + G_{Rx}(\varphi_b) \quad (8)$$

where $G_{Tx}(\varphi_{a,b})$ and $G_{Rx}(\varphi_{a,b})$ are the losses due to angles of the diffracted wave leaving the transmit antenna and coming into the receive antenna, for sides a and b, respectively. L_{diff_sidea} and L_{diff_sideb} are the total diffraction loss around each side found using the method of Recommendation ITU-R P.526 for double isolated edges.

3.2.1.3 Calculation of the ground reflected component

It is assumed that the path is sufficiently short that the ground reflected wave may be modelled by the geometry shown in Fig. 6.

FIGURE 6

Ground reflected component

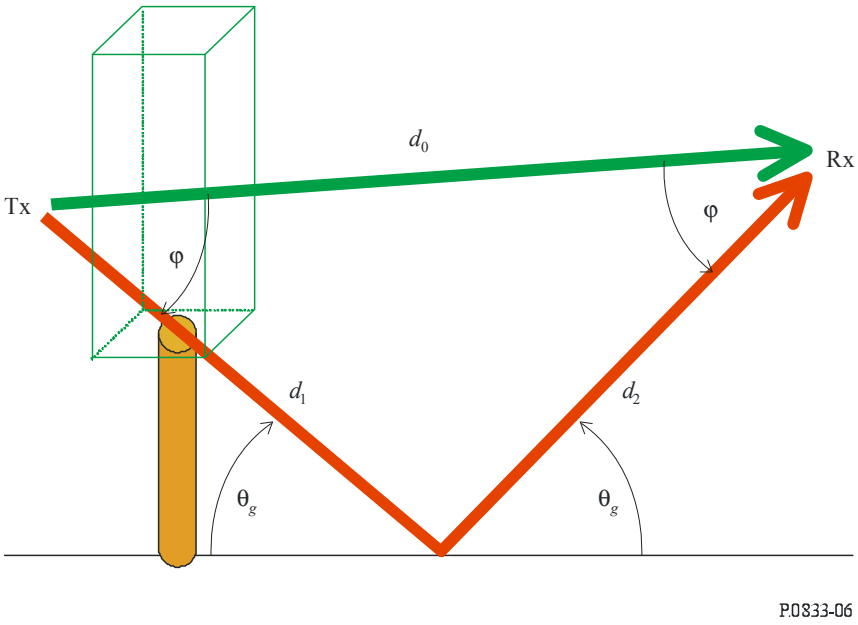

To calculate the loss experienced by the ground reflected wave at the receiver, the reflection coefficient, R_0, of the ground reflected signal may be calculated with a given grazing angle, θ_g. This is a standard method and is described in Recommendation ITU-R P.1238. The values for the permittivity and conductance are obtained from Recommendation ITU-R P.527.

The loss experienced by the ground reflected wave, L_{ground}, is then given by:

$$L_{ground} = 20 \log_{10}\left(\frac{d_1 + d_2}{d_0}\right) - 20 \log_{10}(R_0) + G_{Tx}(\varphi) + G_{Rx}(\varphi) \quad (9)$$

where $G_{Rx}(\varphi)$ and $G_{Tx}(\varphi)$ are the losses due to angles of the reflected wave leaving the transmit antenna and coming into the receive antenna, respectively.

3.2.1.4 Calculation of the "through" or scattered component

In order to make accurate predictions of the excess attenuation to vegetation the user needs to input the following parameters into the RET equation (equation (10)):

α: ratio of the forward scattered power to the total scattered power

β: beamwidth of the phase function (degrees)

σ_τ: combined absorption and scatter coefficient

W: albedo

$\Delta\gamma_R$: beamwidth of the receiving antenna (degrees)

d: distance into the vegetation (m).

Given the input parameters: frequency (GHz), the typical leaf size of the vegetation to be modelled and the leaf area index (LAI) of the tree species, one can obtain the nearest value of α, β, W and σ_τ from the RET parameter tables (Tables 3-6). Should these parameters be unavailable, one should assume the nearest match from the species listed to the Tables.

These four tabled parameters, together with the frequency, and $\Delta\gamma_{3dB}$, the 3 dB beamwidth of the receive antenna, are then used in the RET model.

The attenuation due to scatter through the vegetation, L_{scat}, is then given by:

$$L_{scat} = -10 \log_{10} \left(\begin{array}{l} e^{-\tau} + \frac{\Delta\gamma_R^2}{4} \cdot \{[e^{-\hat{\tau}} - e^{-\tau}] \cdot \bar{q}_M + e^{-\tau} \cdot \sum_{m=1}^{M} \frac{1}{m!} (\alpha W \tau)^m \ [\bar{q}_m - \bar{q}_M]\} \\ + \frac{\Delta\gamma_R^2}{2} \cdot \{-e^{-\hat{\tau}} \cdot \frac{1}{P_N} + \sum_{k=\frac{N+1}{2}}^{N} [A_k e^{\frac{\hat{\tau}}{s_k}} \cdot \frac{1}{1 - \frac{\mu_N}{s_k}}]\} \end{array} \right) \quad (10)$$

where:

$\Delta\gamma_R = 0.6 \cdot \Delta\gamma_{3dB}$: 3 dB beamwidth of the receiving antenna

m: order of the first term I_1 will not change significantly for $m > 10$ (hence for most cases, $M = 10$)

$\tau = (\sigma_a + \sigma_s) \cdot z$: optical density τ as function of distance z.

$$\bar{q}_m = \frac{4}{\Delta\gamma_R^2 + m\beta_S^2}$$

$$\beta_S = 0.6 \cdot \beta$$

$$P_N = \sin^2\left(\frac{\pi}{2N}\right) \quad (11)$$

$$\hat{\tau} = (1 - \alpha W)\tau$$

The attenuation coefficients, s_k, are determined by the characteristic equation:

$$\frac{\hat{W}}{2} \cdot \sum_{n=0}^{N} \frac{P_n}{1 - \frac{\mu_n}{s}} = 1$$

where:

$$P_n = \sin\left(\frac{\pi}{N}\right) \sin\left(\frac{n\pi}{N}\right), (n = 1, \ldots, N\text{-}1), \text{ and } \hat{W} = \frac{(1 - \alpha)W}{1 - \alpha W} \quad (12)$$

where N is an odd integer chosen as a compromise for computing time. Large values of N will dramatically increase computation time. Reasonable values have been determined as $11 \leq N \leq 21$. The left hand side of (10) will be equal to 1 for values of s, which represent the roots of this equation. It will yield $N + 1$ roots, for which the following applies:

$$S_{0,\ldots,\frac{N}{2}} = -S_{N,\ldots,\frac{N+1}{2}}$$

The amplitude factors, A_k, are determined by a system of linear equations given by:

$$\sum_{k=\frac{N+1}{2}}^{N} \frac{A_k}{1-\frac{\mu_n}{s_k}} = \frac{\delta_n}{P_N} \qquad \text{for } n = \frac{N+1}{2} \ldots . N \tag{13}$$

where:

$$\mu_n = -\cos\left(\frac{n\pi}{N}\right)$$

$$\delta_n = 0 \quad \text{for } n \neq N$$

and

$$\delta_n = 1 \quad \text{for } n = N$$

3.2.1.5 Combination of the individual components

The total loss, L_{total}, experienced by a signal propagating through trees is then given by the combination of loss terms:

$$L_{total} = -10 \log_{10}\left\{10^{\left(\frac{-L_{sidea}}{10}\right)} + 10^{\left(\frac{-L_{sideb}}{10}\right)} + 10^{\left(\frac{-L_{top}}{10}\right)} + 10^{\left(\frac{-L_{ground}}{10}\right)} + 10^{\left(\frac{-L_{scat}}{10}\right)}\right\} \tag{14}$$

TABLE 2

Vegetation parameters

	Horse chestnut	Silver maple		London plane		Common lime		Sycamore maple	
	In leaf	In leaf	Out of leaf	In leaf	Out of leaf	In leaf	Out of leaf	In leaf	Out of leaf
LAI		1.691		1.930		1.475		1.631	0.483
Leaf size (m)	0.300	0.150		0.250		0.100		0.150	

	Ginkgo	Cherry, japanese	Trident maple	Korean pine	Himalayan cedar	Plane tree, american	Dawn-redwood
	In leaf	In leaf	Out of leaf	In leaf	In leaf	In leaf	In leaf
LAI	2.08	1.45	1.95				
Leaf size (m)	0.1 × 0.055	0.05 × 0.08	0.07 × 0.085	0.001 × 0.1	0.001 × 0.046	0.22 × 0.16	0.035 × 0.078

Cherry, Japanese: Prunus serrulata var. spontanea
Common lime: Tilia x. Europaea
Dawn redwood: Metasequoia glyptostroboides
Ginkgo: Ginkgo biloba
Horse chestnut: Aesculus hippocastanum L
Himalayan cedar: Cedrus deodara
London plane: Plantanus hispanica muenchh
Korean pine: Pinus Koraiensis
Plane tree, American: Platanus occidentalis
Silver maple: Acer saccharinum L
Sycamore maple: Acer pseudoplatanus L
Trident maple: Acer buergerianum

TABLE 3

Fitted values of α with frequency/species

Frequency (GHz)	Horse chestnut	Silver maple		London plane		Common lime		Sycamore maple	
	In leaf	In leaf	Out of leaf	In leaf	Out of leaf	In leaf	Out of leaf	In leaf	Out of leaf
1.3	0.90	0.95	0.90	0.95	0.90	0.90	0.95		0.95
2	0.75		0.95	0.95			0.95		0.95
2.2			0.95	0.50					
11	0.85	0.90		0.70	0.95	0.95	0.95		0.95
37				0.95					
61.5		0.80		0.25				0.90	

Frequency (GHz)	Ginkgo	Cherry, Japanese	Trident maple	Korean pine	Himalayan cedar	Plane tree, american	Dawn-redwood
	In leaf	In leaf	In leaf	In leaf	In leaf	In leaf	In leaf
1.5	0.90	0.95	0.95	0.70	0.48	0.95	0.93
2.5	0.90	0.93	0.95	0.82	0.74	0.74	0.82
3.5	0.30	0.90	0.95	0.74	0.92	0.85	0.85
4.5	0.40	0.90	0.90	0.72	0.91	0.75	0.89
5.5	0.40	0.95	0.90	0.73	0.96	0.70	0.82
12.5	0.20	0.16	0.25	0.23	0.27	0.71	0.21

NOTE – Leaf size in metres.

TABLE 4

Fitted values of β with frequency/species

Frequency (GHz)	Horse chestnut	Silver maple		London plane		Common lime		Sycamore maple	
	In leaf	In leaf	Out of leaf	In leaf	Out of leaf	In leaf	Out of leaf	In leaf	Out of leaf
1.3	21	14	43	42	16	76	50		70
2	80		31	49			60		62
2.2			25	13					
11	69	58		100	19	78	48		44
37				18					
61.5		48		2				59	

Frequency (GHz)	Ginkgo	Cherry, Japanese	Trident maple	Korean pine	Himalayan cedar	Plane tree, american	Dawn-redwood
	In leaf	In leaf	In leaf	In leaf	In leaf	In leaf	In leaf
1.5	28.65	57.30	18.47	70	51.5	61	44
2.5	36.89	57.30	45.34	55	77.5	23	71
3.5	57.30	114.59	13.43	72	103	105	65
4.5	28.65	114.59	57.30	71	94	65	34
5.5	28.65	229.18	114.59	75	100	77	77
12.5	3.58	3.38	4.25	4.37	3.54	2.36	2.57

NOTE – Leaf size in metres.

TABLE 5

Fitted values of albedo with frequency/species

Frequency (GHz)	Horse chestnut	Silver maple		London plane		Common lime		Sycamore maple	
	In leaf	In leaf	Out of leaf	In leaf	Out of leaf	In leaf	Out of leaf	In leaf	Out of leaf
1.3	0.25	0.95	0.25	0.95	0.95	0.95	0.95		0.85
2	0.55		0.95	0.95			0.95		0.95
2.2			0.95	0.45					
11	0.95	0.95		0.95	0.95	0.75	0.95		0.95
37				0.95					
61.5		0.80		0.50				0.90	

Frequency (GHz)	Ginkgo	Cherry, japanese	Trident maple	Korean pine	Himalayan cedar	Plane tree, american	Dawn-redwood
	In leaf	In leaf	In leaf	In leaf	In leaf	In leaf	In leaf
1.5	0.95	0.95	0.96	0.78	0.43	0.88	0.98
2.5	0.92	0.95	0.95	0.92	0.71	0.71	0.97
3.5	0.10	0.95	0.95	0.71	0.87	0.84	0.93
4.5	0.83	0.30	0.95	0.87	0.92	0.95	0.99
5.5	0.90	0.90	0.95	0.75	0.97	0.96	0.94
12.5	0.97	0.90	0.94	0.98	0.98	0.25	0.99

NOTE – Leaf size in metres.

TABLE 6

Fitted values of σ_τ with frequency/species

Frequency (GHz)	Horse chestnut	Silver maple		London plane		Common lime		Sycamore maple	
	In leaf	In leaf	Out of leaf	In leaf	Out of leaf	In leaf	Out of leaf	In leaf	Out of leaf
1.3	0.772	0.241	0.139	0.147	0.221	0.22	0.591		0.360
2	0.091		0.176	0.203			0.692		0.249
2.2			0.377	0.244					
11	0.124	0.321		0.750	0.459	0.56	0.757		0.179
37				0.441					
61.5		0.567		0.498				0.647	

Frequency (GHz)	Ginkgo	Cherry, Japanese	Trident maple	Korean pine	Himalayan cedar	Plane tree, american	Dawn-redwood
	In leaf	In leaf	In leaf	In leaf	In leaf	In leaf	In leaf
1.5	0.40	0.30	0.47	0.215	0.271	0.490	0.261
2.5	1.10	0.49	0.73	0.617	0.402	0.486	0.350
3.5	0.30	0.21	0.73	0.334	0.603	0.513	0.370
4.5	0.46	0.20	0.27	0.545	0.540	0.691	0.266
5.5	0.48	0.24	0.31	0.310	0.502	0.558	0.200
12.5	0.74	0.18	0.47	0.500	0.900	0.170	0.440

Note: Leaf size in meters.

FIGURE 7

Attenuation for 0.5 m^2 and 2 m^2 illumination area, a) in leaf, b) out of leaf)*

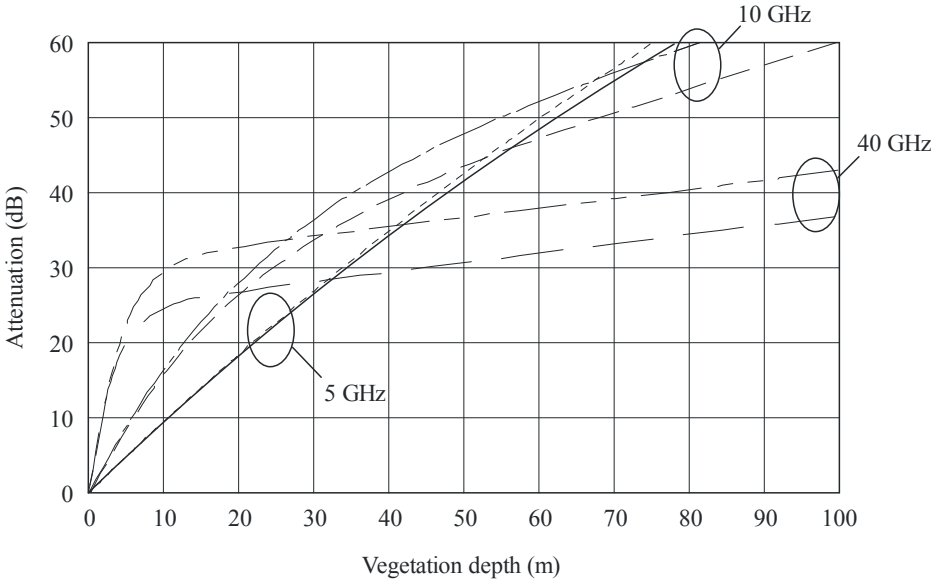

a)

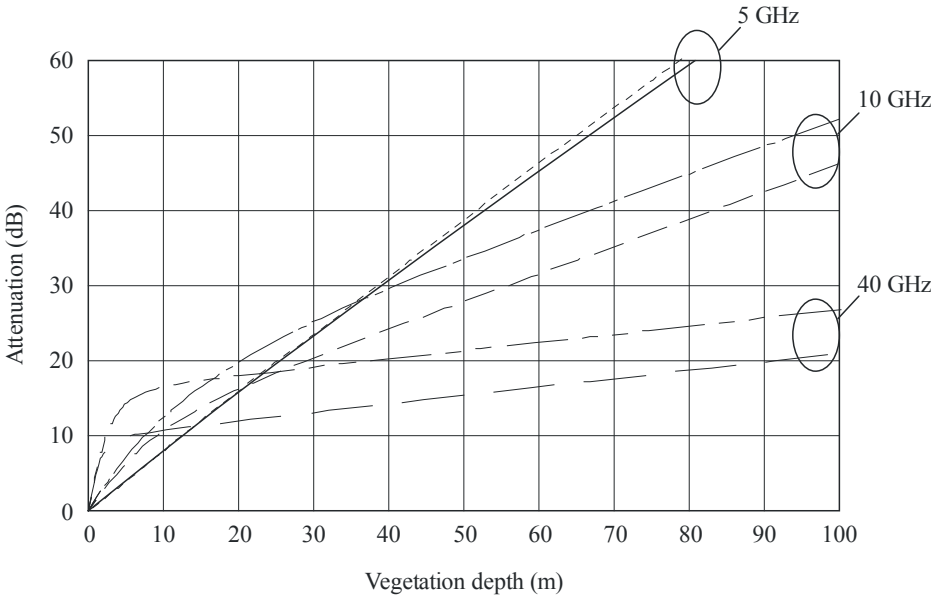

b)

5 GHz, 0.5 m^2
5 GHz, 2 m^2
10 GHz, 0.5 m^2
10 GHz, 2 m^2
40 GHz, 0.5 m^2
40 GHz, 2 m^2

* The curves show the excess loss due to the presence of a volume of foliage which will be experienced by the signal passing through it. In practical situations the signal beyond such a volume will receive contributions due to propagation both through the vegetation and diffracting around it. The dominant propagation mechanism will then limit the total vegetation loss.

P.0833-07

3.2.2 Slant path

For slant paths, it is recommended that the following step-by-step method should be used to compute the total loss due to the tree, the Rice factor and the small-scale cumulative distribution of received power.

The model input parameters are (see Fig. 8 for geometry definition):

R: radius of the canopy (metres)

H: height of the canopy (metres)

θ_i: incident elevation angle to the canopy (radians)

φ_i: incident azimuth angle to the canopy (radians)

φ_s: azimuth scattering angle (radians)

f: frequency (GHz, between 1 and 100 GHz)

d_{TRx}: horizontal distance from the receive antenna to the tree (metres)

h_T: height of the canopy base (meters)

h_{Rx}: height of the receive antenna (metres, must be less than $h_T + H/2$)

link polarization (*V*, *H*, *RHCP* or *LHCP*).

FIGURE 8

Geometry definition

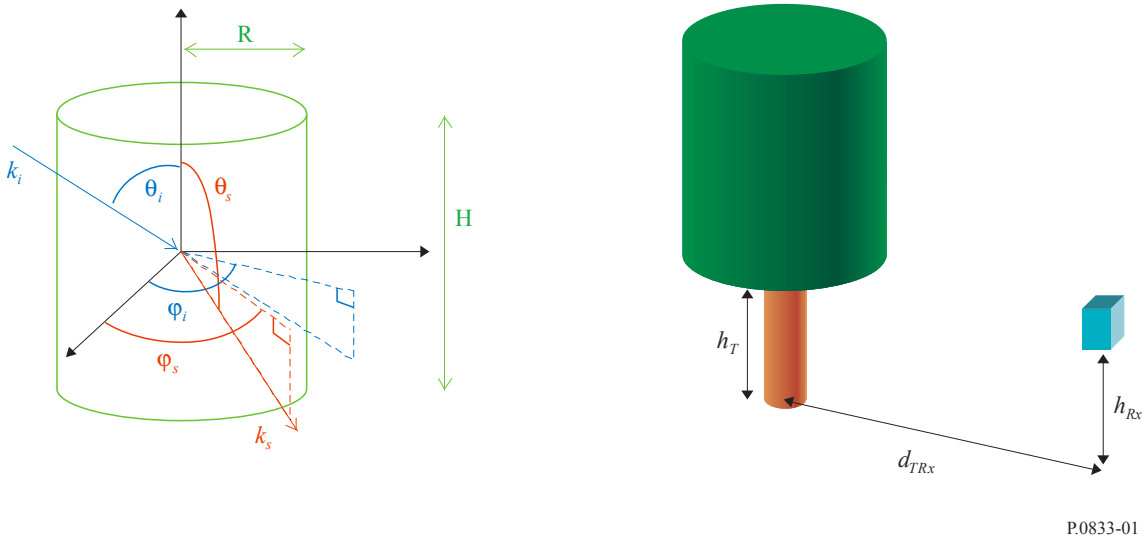

Step 1 Compute θ_s, the elevation scattering angle (in radian):

$$\theta_s = \frac{\pi}{2} - \tan 2^{-1}\left(h_{Rx} - \left(h_T + \frac{H}{2}\right), d_{TRx}\right) \tag{15}$$

Step 2 Define the characteristics of branches and leaves:

a: radius (m)

h: length (m)

ε_r: dielectric constant

ρ: density (m^{-3}).

If a, h and ρ are unknown, use the values given in Table 7 corresponding to a typical oak tree.

TABLE 7

Measured size and density of branches and leaves of an oak tree in Boxtel, the Netherlands

Scatterer type	Radius (cm)	Length/thickness (cm)	Number density (m^{-3})
Branch (1)	11.4	131	0.013
Branch (2)	6.0	99	0.073
Branch (3)	2.8	82	0.41
Branch (4)	0.7	54	5.1
Branch (5)	0.2	12	56
Leaf	3.7	0.02	420

If the dielectric constant for branches and leaves are unknown, they can be computed in the following way:

– leaves:

$$\varepsilon_l = 3.1686 + \frac{28.938}{1 + j\frac{f}{18}} - j\frac{0.5672}{f} \tag{16}$$

– branches:

$$\varepsilon_b = \varepsilon_b' \left(1 + j \tan \delta_b\right) \tag{17}$$

where ε'_b and $\tan \delta_b$ are computed at frequency f by linear interpolation of the values given in Table 8.

TABLE 8

Dielectric constant and loss tangent of wood for moisture content = 40% and temperature = 20°C

Freq (GHz)	1	2.4	5.8	100
ε'_b	7.2	6.2	6.0	5.3
$\tan \delta_b$	0.29	0.30	0.37	0.43

Step 3 Define the wavelength λ (in metres):

$$\lambda = \frac{0.3}{f} \tag{18}$$

Step 4 For each category of branches and for the category of leaves, compute the scattering amplitude tensors for the following values of azimuth and elevation orientation of the branches and leaves:

Azimuth: $\varphi_{sc}(i_\varphi) = i_\varphi \frac{2\pi}{5}$ with $0 \le i_\varphi \le 5$

Elevation: $\theta_{sc}(i_\theta) = i_\theta \frac{\beta_{max}}{5}$ with $0 \le i_\theta \le 5$ where $\beta_{max} = \pi/4$ for branches of categories (1) and (2) and $\beta_{max} = \pi/2$ for branches of category (3), (4), (5) and leaves.

Step 4.1 Compute the incidence and departure angles in the scatterer local frame $\theta_{i,sc}$, $\varphi_{s,sc}$, $\theta_{s,sc}$ and $\varphi_{s,sc}$.

$$\begin{cases} \theta_{i,sc} = \cos^{-1}\left(\cos\theta_{sc}\cos\theta_i - \sin\theta_{sc}\cos(\varphi_{sc} - \varphi_i)\sin\theta_i\right) \\ \varphi_{i,sc} = \tan 2^{-1}\left(\sin\theta_i \sin(\varphi_i - \varphi_{sc}), \sin\theta_i \cos\theta_{sc}\cos(\varphi_{sc} - \varphi_i) + \sin\theta_{sc}\cos\theta_i\right) \\ \theta_{s,sc} = \pi - \cos^{-1}\left(-\cos\theta_{sc}\cos\theta_s - \sin\theta_{sc}\cos(\varphi_{sc} - \varphi_s)\sin\theta_s\right) \\ \varphi_{i,sc} = \tan 2^{-1}\left(\sin\theta_s \sin(\varphi_s - \varphi_{sc}), \sin\theta_s \cos\theta_{sc}\cos(\varphi_{sc} - \varphi_s) + \sin\theta_{sc}\cos\theta_s\right) \end{cases} \quad (19)$$

Step 4.2 Compute the local frame amplitude scattering tensors f_{vv}, f_{vh}, f_{hv} and f_{hh} for each category of branches and leaves:

– Branches for which $\left|\frac{2\pi}{\lambda} a\sqrt{\varepsilon_r} - 1\right| < 1$ and leaves:

$$\begin{cases} f_{vv} = \dfrac{\left(\frac{2\pi}{\lambda}\right)^2 (\varepsilon_r - 1)}{2}\left(a_N \sin\theta_{i,sc}\sin\theta_{s,sc} - a_T \cos\theta_{i,sc}\cos\theta_{s,sc}\cos(\varphi_{s,sc} - \varphi_{i,sc})\right)\mu \\ f_{hv} = \dfrac{\left(\frac{2\pi}{\lambda}\right)^2 (\varepsilon_r - 1)}{2} a_T \cos\theta_{i,sc}\sin(\varphi_{s,sc} - \varphi_{i,sc})\mu \\ f_{hh} = \dfrac{\left(\frac{2\pi}{\lambda}\right)^2 (\varepsilon_r - 1)}{2} a_T \cos(\varphi_{s,sc} - \varphi_{i,sc})\mu \\ f_{vh} = \dfrac{\left(\frac{2\pi}{\lambda}\right)^2 (\varepsilon_r - 1)}{2} a_T \cos\theta_{s,sc}\sin(\varphi_{s,sc} - \varphi_{i,sc})\mu \end{cases} \quad (20)$$

with

$$\begin{cases} a_T = \dfrac{1}{(\varepsilon_r - 1)g_t + 1} \\ a_N = \dfrac{1}{(\varepsilon_r - 1)g_n + 1} \end{cases} \quad (21)$$

where:

– Branches:

$$\begin{cases} b = \sqrt{1 - \left(\dfrac{2a}{h}\right)^2} \\ g_t = \dfrac{b\left(b^2 - 1\right)}{2}\left(\dfrac{b}{b^2 - 1} + \dfrac{\log_{10}\dfrac{b-1}{b+1}}{2}\right) \\ g_n = -\left(b^2 - 1\right)\left(\dfrac{b\log_{10}\dfrac{b-1}{b+1}}{2} + 1\right) \end{cases} \tag{22}$$

– Leaves:

$$\begin{cases} m = \dfrac{2a}{h} \\ g_t = \dfrac{1}{2\left(m^2 - 1\right)}\left(\dfrac{m^2}{\sqrt{m^2 - 1}}\sin^{-1}\left(\dfrac{\sqrt{m^2 - 1}}{m}\right) - 1\right) \\ g_n = \dfrac{m^2}{m^2 - 1}\left(1 - \dfrac{1}{\sqrt{m^2 - 1}}\sin^{-1}\left(\dfrac{\sqrt{m^2 - 1}}{m}\right)\right) \end{cases} \tag{23}$$

$$\mu = \sum_{n-5}^{5}\sum_{l=0}^{50}\sum_{p=0}^{50}\left[l\frac{a}{50}J_n\left(\frac{2\pi}{\lambda}l\frac{a}{50}\sin\theta_{i,sc}\right)J_n\left(\frac{2\pi}{\lambda}l\frac{a}{50}\sin\theta_{s,sc}\right) \times \exp\left(j\frac{2\pi}{\lambda}h\left(\frac{l}{50} - \frac{1}{2}\right)\right)\left(\cos\theta_{i,sc} + \cos\theta_{s,sc}\right)\frac{a}{50}\frac{h}{50}\right] \tag{24}$$

– Branches for which $\left|\dfrac{2\pi}{\lambda}a\sqrt{\varepsilon_r} - 1\right| > 1$

$$\begin{cases} f_{vv} = \left(\dfrac{2\pi}{\lambda}\right)^2(\varepsilon_r - 1)h\mu\left(\dfrac{E_v(0)\left(Z(-1) + Z(1)\right)\cos\theta_{i,sc}\cos\theta_{s,sc}}{2\sqrt{\varepsilon_r - \cos^2\theta_{i,sc}}} - Z(0)\sin\theta_{s,sc} + G_{vv}\right) \\ f_{vh} = 2j\left(\dfrac{2\pi}{\lambda}\right)^2(\varepsilon_r - 1)h\mu\left(\dfrac{E_v(0)\left(Z(-1) + Z(1)\right)\cos\theta_{i,sc}\cos\theta_{s,sc}}{2\sqrt{\varepsilon_r - \cos^2\theta_{i,sc}}} - Z(0)\sin\theta_{s,sc} + G_{vh}\right) \\ f_{hh} = \left(\dfrac{2\pi}{\lambda}\right)^2(\varepsilon_r - 1)h\mu\left(\dfrac{H_h(0)\left(Z(-1) + Z(1)\right)}{2\sqrt{\varepsilon_r - \cos^2\theta_{i,sc}}} + G_{hh}\right) \\ f_{vh} = j\left(\dfrac{2\pi}{\lambda}\right)^2(\varepsilon_r - 1)h\mu G_{hv} \end{cases} \tag{25}$$

with:

$$\mu = \frac{\sin\frac{2\pi}{\lambda} h\left(\cos\theta_{i,sc} + \cos\theta_{s,sc}\right)}{\frac{2\pi}{\lambda} h\left(\cos\theta_{i,sc} + \cos\theta_{s,sc}\right)} \tag{26}$$

$$Z(n) = \frac{a^2}{u^2 - v_s^2}\left(uJ_n(v_s)J_{n+1}(u) - v_s J_n(u)J_{n+1}(v_s)\right) \tag{27}$$

$$\begin{cases} G_{vv} = 2\sum_{n=1}^{20}\left(\beta(n)E_v(n)\cos\theta_{i,sc} - j\alpha(n)H_v(n)\cos\theta_{s,sc} - Z(n)E_v(n)\sin\theta_{s,sc}\right)\cos\left(n\left(\varphi_{s,sc} - \varphi_{i,sc}\right)\right) \\ G_{vh} = 2\sum_{n=1}^{20}\left(\beta(n)E_h(n)\cos\theta_{i,sc} - j\alpha(n)H_h(n)\cos\theta_{s,sc} - Z(n)E_v(n)\sin\theta_{s,sc}\right)\sin\left(n\left(\varphi_{s,sc} - \varphi_{i,sc}\right)\right) \\ G_{hh} = 2\sum_{n=1}^{20}\left(\beta(n)H_h(n) + j\alpha(n)E_h(n)\cos\theta_{i,sc}\right)\cos\left(n\left(\varphi_{s,sc} - \varphi_{i,sc}\right)\right) \\ G_{vv} = 2\sum_{n=1}^{20}\left(\beta(n)H_v(n) + j\alpha(n)E_v(n)\cos\theta_{i,sc}\right)\sin\left(n\left(\varphi_{s,sc} - \varphi_{i,sc}\right)\right) \end{cases} \tag{28}$$

where:

$$\begin{cases} u = \frac{2\pi}{\lambda} a\sqrt{\varepsilon_r - \cos^2\theta_{i,sc}} \\ v_i = \max\left(10^{-5}, \frac{2\pi}{\lambda} a\sin\theta_{i,sc}\right) \\ v_s = \frac{2\pi}{\lambda} a\sin\theta_{s,sc} \end{cases} \tag{29}$$

$$\begin{cases} \alpha(n) = \dfrac{Z(n-1) - Z(n+1)}{2\sqrt{\varepsilon_r - \cos^2\theta_{i,sc}}} \\ \beta(n) = \dfrac{Z(n-1) + Z(n+1)}{2\sqrt{\varepsilon_r - \cos^2\theta_{i,sc}}} \end{cases} \tag{30}$$

$$\begin{cases} E_v(n) = \dfrac{j\sin\theta_{i,sc}}{R(n)J_n(u)}\left(\dfrac{H'(n)}{v_i H_n^{(2)}(v_i)} - \dfrac{J'(n)}{uJ_n(u)}\right) \\ E_h(n) = \dfrac{-\sin\theta_{i,sc}}{R(n)J_n(u)}\left(\dfrac{1}{v_i^2} - \dfrac{1}{u^2}\right)n\cos\theta_{i,sc} \\ H_v(n) = \dfrac{\sin\theta_{i,sc}}{R(n)J_n(u)}\left(\dfrac{1}{v_i^2} - \dfrac{1}{u^2}\right)n\cos\theta_{i,sc} \\ H_h(n) = \dfrac{j\sin\theta_{i,sc}}{R(n)J_n(u)}\left(\dfrac{H'(n)}{v_i H_n^{(2)}(v_i)} - \varepsilon_r\dfrac{J'(n)}{uJ_n(u)}\right) \end{cases} \tag{31}$$

$$\begin{cases} J^{'}(n) = \dfrac{J_{n-1}(u) - J_{n+1}(u)}{2} \\ H^{'}(n) = \dfrac{H^{(2)}_{n-1}(v_i) - H^{(2)}_{n+1}(v_i)}{2} \\ R(n) = \dfrac{\pi v_i^2 H_n^{(2)}}{2}\left(\left(\dfrac{H^{'}(n)}{v_i H_n^{(2)}(v_i)} - \dfrac{J^{'}(n)}{uJ_n(u)}\right)\left(\dfrac{H^{'}(n)}{v_i H_n^{(2)}(v_i)} - \varepsilon_r \dfrac{J^{'}(n)}{uJ_n(u)}\right) - \left(\dfrac{1}{u^2} - \dfrac{1}{v_i^2}\right) n \cos\theta_{i,sc}\right) \end{cases} \quad (32)$$

$J_n(.)$ being the n^{th} order Bessel function of the first kind

$H_n^{(2)}(.)$ being the n^{th} order Hankel function

Step 4.3 Compute the frame rotation factors:

$$\begin{cases} t_{vi} = -(\sin\theta_{sc}\cos\theta_i\cos(\varphi_{sc} - \varphi_i) + \cos\theta_{sc}\sin\theta_i) \\ t_{hi} = \sin\theta_{sc}\sin(\varphi_{sc} - \varphi_i) \\ t_{vs} = \sin\theta_{sc}\cos\theta_s\cos(\varphi_{sc} - \varphi_s) - \cos\theta_{sc}\sin\theta_s \\ t_{hs} = \sin\theta_{sc}\sin(\varphi_{sc} - \varphi_s) \end{cases} \quad (33)$$

Step 4.4 Compute the reference frame scattering tensors matrix F_{VV}, F_{VH}, F_{HV} and F_{HH} for each category of branches and leaves:

$$\begin{cases} F_{VV} = \dfrac{1}{\sqrt{(t_{vi}^2 + t_{hi}^2)(t_{vs}^2 + t_{hs}^2)}}\left[t_{vs}(f_{vv}t_{vi} - f_{vh}t_{hi}) - t_{hs}(f_{hv}t_{vi} - f_{hh}t_{hi})\right] \\ F_{HH} = \dfrac{1}{\sqrt{(t_{vi}^2 + t_{hi}^2)(t_{vs}^2 + t_{hs}^2)}}\left[t_{hs}(f_{vv}t_{hi} + f_{vh}t_{vi}) + t_{vs}(f_{hv}t_{hi} + f_{hh}t_{vi})\right] \\ F_{HV} = \dfrac{1}{\sqrt{(t_{vi}^2 + t_{hi}^2)(t_{vs}^2 + t_{hs}^2)}}\left[t_{hs}(f_{vv}t_{vi} - f_{vh}t_{hi}) + t_{vs}(f_{hv}t_{vi} - f_{hh}t_{hi})\right] \\ F_{VH} = \dfrac{1}{\sqrt{(t_{vi}^2 + t_{hi}^2)(t_{vs}^2 + t_{hs}^2)}}\left[t_{vs}(f_{vv}t_{hi} + f_{vh}t_{vi}) - t_{hs}(f_{hv}t_{hi} + f_{hh}t_{vi})\right] \end{cases} \quad (34)$$

Step 4.5 Compute the reference frame amplitude scattering tensor $F_{scat}(i_\theta, i_\varphi)$ for the link polarization for each category of branches and leaves:

$$\begin{aligned} &\text{Vertical polarization} && F_{scat}(i_\theta, i_\varphi) = F_{VV} \\ &\text{Horizontal polarization} && F_{scat}(i_\theta, i_\varphi) = F_{HH} \\ &\text{Right Hand Circular Polarization} && F_{scat}(i_\theta, i_\varphi) = \frac{1}{2}\left[F_{VV} + F_{HH} + j(-F_{VH} + F_{HV})\right] \\ &\text{Left Hand Circular Polarization} && F_{scat}(i_\theta, i_\varphi) = \frac{1}{2}\left[F_{VV} + F_{HH} + j(F_{VH} - F_{HV})\right] \end{aligned} \quad (35)$$

Step 5 For each category of branches and leaves, compute the first and the second moments of the scattering amplitude:

$$E\left[\left|F_{scat}\right|^2\right]_{b,l} = \int_0^{2\pi}\int_0^{\beta_{max}} \left|F_{scat}(\theta,\varphi)\right|^2 \frac{\sin\theta}{1-\cos\beta_{max}} d\theta d\varphi \tag{36}$$

where $\int_0^{2\pi}\int_0^{\beta_{max}} f(\theta,\varphi)d\theta d\varphi$ is computed using the trapezoidal rule considering:

$$\int_a^b f(x)dx = \frac{\Delta x}{2}\sum_{k=1}^{N-1}\left(f(x_{k+1}) - f(x_k)\right)$$

$$F_{scat}(\theta,\varphi) = F_{scat}(i_\theta, i_\varphi)$$

$$\Delta\theta = \frac{\beta_{max}}{N_\theta - 1}$$

$$\Delta\varphi = \frac{2\pi}{N_\varphi - 1}$$

$$N_\theta = N_\varphi = 20$$

Step 6 Repeat *Steps 4.1* to *4.5* using $\theta_s = \pi - \theta_i$ and $\varphi_s = \varphi_i$ to compute

$$E\left[F_{scat}\right]_{b,l} = \int_0^{2\pi}\int_0^{\beta_{max}} F_{scat}(\theta,\varphi)\frac{\sin\theta}{1-\cos\beta_{max}} d\theta d\varphi \tag{37}$$

Step 7 Compute the equivalent scattering amplitude and the equivalent scattering cross-section per unit volume of the canopy:

$$F^{eq} = \sum_{branches\ \&\ leaves} \rho_{b,l} E\left[F_{scat}\right]_{b,l} \tag{38}$$

$$\sigma^{eq} = \sum_{branches\ \&\ leaves} 4\pi\rho_{b,l} E\left[\left|F_{scat}\right|^2\right]_{b,l} \tag{39}$$

Step 8 Compute the imaginary part of the effective propagation constant inside the canopy, K_c''

$$K_c'' = -imag\left(\frac{2\pi}{\lambda}\sin\theta_i + \frac{\lambda}{\sin\theta_i} F^{eq}\right) \tag{40}$$

Step 9 Compute the specific attenuation of the tree canopy in decibels per metre (dB/m):

$$\alpha_c = 20K_c'' \log_{10} e = 8.686K_c'' \tag{41}$$

Step 10 Compute the diffuse multipath power relative to the line-of-sight level, $mp = 2\sigma^2$:

$$mp = 2\sigma^2 = \frac{\sigma^{eq}}{4\pi s^2} \int_{-H/2}^{H/2} \int_{-R}^{R} \int_{-R}^{R} \exp(-2K_c''(s_1(x,y,z) + s_2(x,y,z))dxdydz \quad (42)$$

where $\int_{-H/2}^{H/2} \int_{-R}^{R} \int_{-R}^{R} f(x,y,z)dxdydz$ is computed using the trapezoidal rule considering:

$$\begin{cases} s_1(x,y,z) = s_{1,0}(x,y,z) \times \min\left(1, \dfrac{\dfrac{H}{2} - z}{s_{1,0}(x,y,z)\cos\theta_i}\right) & \text{if} \quad x^2 + y^2 \le R^2 \\ s_1(x,y,z) = 0 & \text{if} \quad x^2 + y^2 > R^2 \end{cases} \quad (43)$$

with $s_{1,0}(x,y,z) = \dfrac{(y\sin\varphi_i - x\cos\varphi_i) + \sqrt{(y\sin\varphi_i - x\cos\varphi_i)^2 - \left(x^2 + y^2 - R^2\right)}}{\sin\theta_i}$ (44)

$$\begin{cases} s_2(x,y,z) = s_{2,0}(x,y,z) \times \min\left(1, \dfrac{-\left(\dfrac{H}{2} + z\right)}{s_{2,0}(x,y,z)\cos\theta_s}\right) & \text{if} \quad x^2 + y^2 \le R^2 \\ s_2(x,y,z) = 0 & \text{if} \quad x^2 + y^2 > R^2 \end{cases} \quad (45)$$

with $s_{2,0}(x,y,z) = \dfrac{(-y\sin\varphi_s + x\cos\varphi_s) + \sqrt{(y\sin\varphi_s - x\cos\varphi_s)^2 - \left(x^2 + y^2 - R^2\right)}}{\sin\theta_s}$ (46)

$$\Delta x = \Delta y = \Delta z = \frac{\lambda}{4}$$

Step 11 Compute the geometric path length through the tree, l_{tree} (m)

Step 11.1 Compute δ:

$$\delta = R^2 - d_{TRx}^2 \sin^2(\varphi_i - \varphi_s) \quad (47)$$

Step 11.2 Compute l_{tree}:

- if $\delta \le 0$: $l_{tree} = 0$
- if $\delta > 0$:

$$l_{tree} = \max\left(0, \min\left(\frac{d_{TRx}\cos(\varphi_i - \varphi_s) + \sqrt{\delta}}{\sin\theta_i}, \frac{h_T - h_{Rx} + H}{\cos\theta_i}\right) - \max\left(\frac{d_{TRx}\cos(\varphi_i - \varphi_s) - \sqrt{\delta}}{\sin\theta_i}, \frac{h_T - h_{Rx}}{\cos\theta_i}\right)\right) \quad (48)$$

Step 12 Compute the direct path power relative to the line-of-sight level, a^2:

$$a^2 = 10^{\frac{-\alpha_c \times l_{tree}}{10}} \tag{49}$$

Step 13 Compute the total path power relative to the line-of-sight level, p_{tot}:

$$p_{tot} = a^2 + 2\sigma^2 \tag{50}$$

Step 14 Compute the Rice factor K (dB):

$$K = 10 \log_{10}\left(\frac{a^2}{2\sigma^2}\right) \tag{51}$$

Step 15 Compute the small-scale power cumulative distribution using the Nakagami-Rice distribution defined in Recommendation ITU-R P.1057:

$$\text{Prob}\,(X > x) = 2 \exp\left(-\frac{a^2}{2\sigma^2}\right) \int_{x/\sigma\sqrt{2}}^{\infty} \nu \exp\left(-\nu^2\right) I_0\left(\frac{2\nu a}{\sigma\sqrt{2}}\right) d\nu \tag{52}$$

4 Depolarization

Previous measurements at 38 GHz suggest that depolarization through vegetation may well be large, i.e. the transmitted cross-polar signal may be of a similar order to the co-polar signal through the vegetation. However, for the larger vegetation depths required for this to occur, the attenuation would be so high that both the co-polar and cross-polar components would be below the dynamic range of the receiver.

5 Dynamic effects

It has been observed that where a link passes through vegetation the received signal amplitude varies rapidly when the vegetation moves. The principle cause of movement is due to wind and measurements at 38 GHz and 42 GHz have demonstrated that there is strong correlation between the amplitude fluctuation rate and wind speed.

When considering the effects of vegetation it is clear that the environment will not remain static. A receiver site may have one or more trees along the signal path that do not give a sufficient mean attenuation to take the received signal level below the system margin. However, it has been found that as the trees move, the signal level varies dynamically over a large range making the provision of a service unfeasible. Several measurements of the signal level through trees, as a function of time, have been made and show an average reduction of the signal level of about 20 dB per tree. Considerable signal variability was found, with frequent drop-outs of up to 50 dB attenuation lasting for around 10 ms.

It is noted that the deep null structure seen in time series measurements can only be produced by the interaction of a number of scattering components within the vegetation. In order to simulate this propagation mechanism, the summed field from a number of scattering sources randomly positioned along a line tangential to the path has been calculated. To give the resultant signal a suitable time variability, the position of each scatterer was varied sinusoidally to simulate the movement of tree branches in the wind. The frequency and extent of the position variability was increased with increasing wind speed. This model was in reasonable agreement with observations.

Modelled time series and the standard deviations of signal amplitude for wind speeds, ranging from 0 to 20 m/s, are presented in Fig. 9 in comparison with measured data.

FIGURE 9

Standard deviation of measured and modelled 40 GHz time series as a function of wind speed

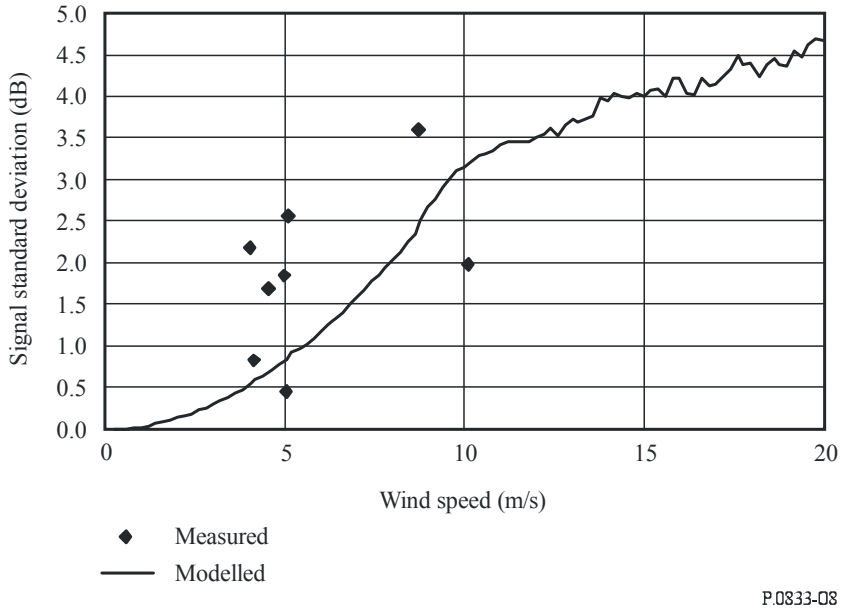

To a simple linear approximation the standard deviation σ is modelled as follows:

$$\sigma = v/4 \qquad \text{dB} \tag{53}$$

where v is the wind speed (m/s).

It should be noted that despite the fact that this type of model shows an inherent frequency dependence, the path length differences through trees are small and the fading across a typical 40 MHz bandwidth will appear flat. Rapid fading is due to the time variability of the medium.

Table 9 presents typical data for mean and standard deviation of attenuation measured at 38 GHz for three tree types under calm conditions and in strong wind.

TABLE 9

Vegetation fade dynamics measured at 38 GHz

Tree type		**Dog-rose bush (diameter of 2 m)**	**Apple tree (diameter of 2.8 m)**	**Pine (diameter of 1.5 m)**
No wind	Mean loss (dB)	8.6	17.4	7.7
	Standard (dB)	2.0	2.8	2.2
Strong wind	Mean loss (dB)	11.7	17.8	12.1
	Standard (dB)	4.4	4.2	4.3

6 Delay-spread characteristics of vegetation

A received signal through vegetation consists of multipath components due to scattering. An input signal suffers delay spread. Delay spread can have a significant effect on wideband digital systems and it is therefore important to be able to predict the delay spread characteristics due to propagation through vegetation.

The data in Table 10 are based on the wideband frequency measurement data from the Republic of Korea. The time-domain characteristics were obtained for a 3.5 GHz carrier signal modulated with a 1.5 ns pulse. The 3 dB bandwidth of the resulting pulse-modulated signal is 0.78 GHz.

TABLE 10

Characteristics of delay through vegetation

Parameters	**Ginkgo**	**Cherry, Japanese**	**Trident maple**	**Korean pine**	**Himalay an cedar**	**Plane tree, american**	**Dawn-redwood**
	In leaf	**In leaf**	**In leaf**	**In leaf**	**In leaf**	**In leaf**	**In leaf**
Vegetation depth (m)	5.4	6.2	4.3	5.2	4.7	6.5	4.7
Delay spread (ns)	7.27	8.23	5.89	6.62	6.39	2.56	6.56